Acta Technica *62* No. 2A/2017, 83–96

Mechanism of TDLAS spectral line distortion and application of calibration technique in time division detection system of optical fiber sensor[1]

Dechun Yuan[2]

Abstract. In order to suppress the emission of harmful gases, gas sensors have come into being. With the development of optical fiber technology, the infrared absorption spectrum gas sensor based on optical fiber has become the focus of discussion. In order to study the application of tunable diode laser absorption spectroscopy (TDLAS) technology in optical fiber sensors, the theoretical analysis of selective absorption of gas molecules was carried out in this paper. By theoretical simulation and experimental verification, the spectral distortions of TDLAS system based on three different demodulation circuits (subtraction circuit, division circuit, BRD circuit) under the influence of non-absorption loss of light intensity were compared. The final experimental results show that different demodulation circuits have different suppression effects on the power fluctuation of laser light source, in which the division demodulation circuit can provide higher detection accuracy.

Key words. TDLAS, spectral line distortion, fiber bending loss.

1. Introduction

Infrared absorption spectrum gas sensor is a rising star of sensor family. However, with its advantages, it has become the focus of discussion in the field of sensing. Until now, infrared absorption spectra of gas sensors have been flourishing. Infrared absorption spectroscopy gas sensing technology has shown many branches. Among them, tunable diode laser absorption spectroscopy (TDLAS) technology is the most widely used and the most representative for real-time gas detection in field. The technique has high measuring accuracy and fast response. The utility model can simultaneously detect a plurality of gas parameters, measure and analyze a plurality of

[1]This work is supported by the Fundamental Research Funds for the Central Universities (Project No.040-41416012).

[2]Northeast Forestry University, Harbin, Heilongjiang, 150040, China; E-mail: 8500284@qq.com

gases. It has wide application range, great potential for development of instruments and long measuring distance. The system has low operating cost, which is easy for installation and upgrade. In addition, the continuous updating and development of optical fiber technology has added new advantages to optical fiber based infrared absorption spectrum gas sensors: low transmission loss of optical fiber, small noise and distortion, high transmission quality. It can realize long-distance light propagation, and remote control telemetry. The optical fiber gas sensor system is easy to connect with the computer, and it can realize multi-function and intelligence. In addition, the fiber transmission band is wide, which is easy to form a sensor network.

2. State of the art

TDLAS technology was first proposed by Hinkley and Reid in 1970s. They modulated the laser output wavelength by modulating the injection current or humidity of the tunable diode laser and applying the technique to the detection of contaminated gas [1]. In 1979, Inaba and Chan of Tohoku University in Japan realized differential absorption gas detection by adjusting the dual output wavelengths of the laser [2]. In 1998, Stewart and others of the University of Strathclyde in England used the space division multiplexing technique to realize multi-point gas detection using a distributed feedback semiconductor laser. The detection limit method was ppmv/m. In addition, they believed that the interference noise in the air chamber was the main factor that limits the signal-to-noise ratio of the system [3]. In 2012, Lei Tao of Princeton University used 4.5 m quantum cascade laser to build a simple and portable free space gas sensor for the simultaneous detection of atmospheric N_2O and CO with the detection accuracy of 0.15 ppbv and 0.36 ppbv, respectively [4]. In 2004, Huang Wei of Anhui Institute of Optics and Fine Mechanics of Chinese Academy of Sciences designed a set of tunable near infrared diode laser spectrometer based on wavelength modulation spectroscopy. Various concentrations of CO_2 were measured in a laboratory combined with a long range absorption cell. When the absorption path was 170 m, the CO_2 with pressure of 1.9995 Pa could be detected. In this low voltage case, the signal-to-noise ratio of the two harmonic was still very high [5]. In 2011, Zhang Ruifeng and others from Tianjin University introduced a remote sensing system for mine gas concentration based on wavelength modulation spectroscopy. A method of determining the burning concentration of a light by detecting the harmonic component of the reflected signal was used to eliminate the influence of the background gas and dust on the attenuation of laser intensity. The minimum detection sensitivity of the system was 0.0714 mg/m^3, and the maximum detection distance could reach 10 m [6].

3. Methodology

Direct absorption spectroscopy (TDLAS) is the simplest and most direct detection technique in the field of gas sensing technology. It allows very primitive and intuitive gas absorption contours. Linear fitting based on gas absorption profile can

not only convenient for researchers to get gas concentration information, but also can get other important environmental parameter information, such as gas and temperature [7]. A typical block diagram of the TDLAS gas sensing system based on direct absorption spectroscopy was shown in Fig. 1.

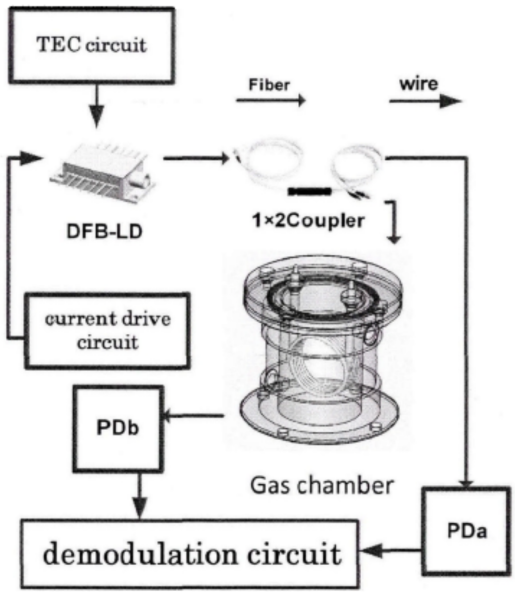

Fig. 1. Detection principle diagram of TDLAS system based on direct absorption spectroscopy

Firstly, the scanning signal (usually sawtooth or triangular wave) is changed by external driving circuit to change the injection current of the laser so as to realize the scanning of the output wavelength of the laser. The output light of the laser is divided into two by an optical fiber coupler. A beam of light passes through the gas chamber and is coupled to the photodetector a, which we call a probe beam. Another beam of light goes directly into the photodetector b as a reference, and we call it a reference beam. Then, the two signals are processed by a differential adjustment circuit to eliminate the scanning baselines brought by the injection current modulation of the laser (current modulation can cause the laser amplitude modulated optical power at the same time), so as to extract the absorption peaks of the tested gas with the zero baseline [8].

There are mainly three kinds of demodulation circuits used in direct absorption spectrum, namely subtraction circuit, division circuit and BRD circuit.

The schematic diagram of the subtraction demodulation circuit is shown in Fig. 2. When the reference beam and the detecting beam are respectively connected by a photoelectric detector, they are converted into a voltage signal through the current and voltage conversion circuit at the same time. Then, after amplifying the proper multiples through the amplifier, the baselines of the two signals are amplified to the same size, and the differential amplifier (subtraction device) is added to the

differential amplifier. The amplified signal finally enters the signal acquisition circuit to be measured (concentration) [9].

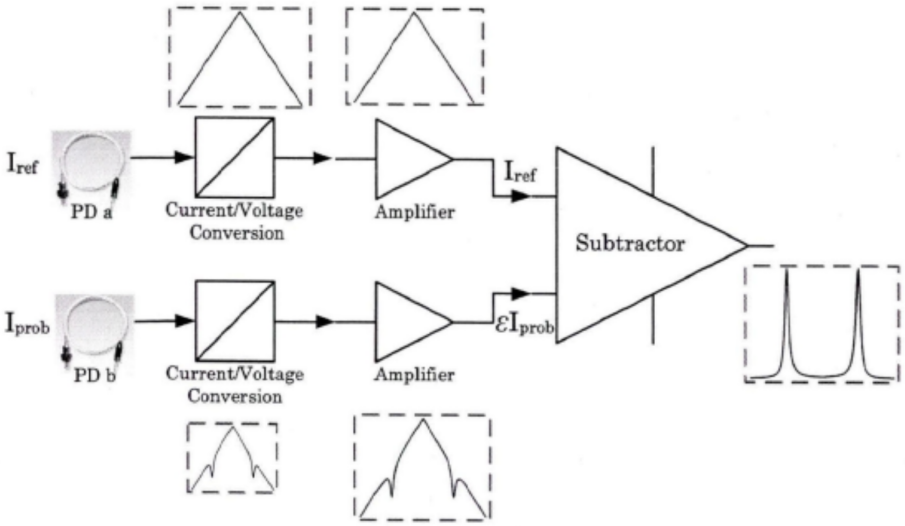

Fig. 2. Schematic diagram of subtraction circuit

According to Fig. 2, it is assumed that the two light intensities coupled to the detector are $I_{\mathrm{ref}}(v)$ and $I_{\mathrm{prob}}(v)$, respectively, as shown in the equations

$$I_{\mathrm{ref}}(v) = I_0(v)\,, \tag{1}$$

$$I_{\mathrm{prob}}(v) = \frac{1}{\varepsilon} I_0(v) \cdot \exp[-\alpha(v)CL]\,. \tag{2}$$

Here, ε is the intensity ratio of reference light to detective light. After the operation amplifier amplifies ε times and the baseline of the probe signal is amplified to the same size as the reference light baseline, as shown in the formula

$$\varepsilon I_{\mathrm{prob}}(v) = I_0(v) \cdot \exp[-\alpha(v)CL]\,. \tag{3}$$

After differential processing, the subtraction device output is shown in the formula

$$I_{\mathrm{out}} = I_{\mathrm{ref}} - \varepsilon I_{\mathrm{prob}} = I_0(v)\,(1 - \exp[-\alpha(v)CL])\ . \tag{4}$$

When $\alpha(v)CL$
$ll1$ and $\exp[-\alpha(v)CL] \approx 1 - \alpha CL$, formula (4) can be converted to formula (5), which is expressed as follows:

$$I_{\mathrm{out}} = I_0(v)\alpha(v)CL\,. \tag{5}$$

When $I_0(v)$ is constant, the output signal $I_{\mathrm{out}}(v)$ is directly proportional to the

concentration of the gas to be measured. Therefore, the concentration of the gas to be measured Ccan be calculated by the peak value of the demodulated absorption peak.

The principal diagram of division circuit is shown in Fig. 3. The principle of division circuit and flow chart of the subtraction circuit are basically the same, but the subtractor replaces the divider. But it should be noted that after the divider, adder subtracter or circuit is needed to adjust the bias. And when the detection light path is as the input of a molecular divider (some division chip output comes out of the inverse function), demodulation absorption peak signal is inverted, which needed to go through the signal processing for reversed phase inverter. Finally, it is sent to the acquisition circuit or computer for signal acquisition [10].

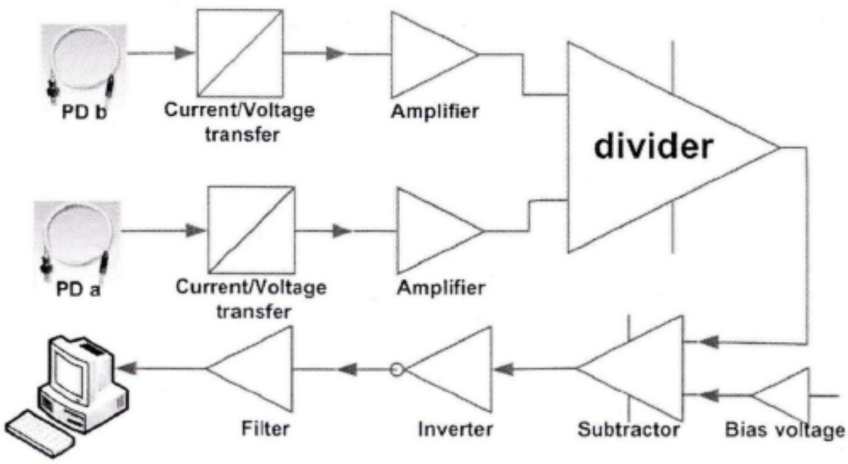

Fig. 3. Principal diagram of division circuit

It is assumed that the two light intensities coupled to the detector remain $I_{\mathrm{ref}}(v)$ and $I_{\mathrm{prob}}(v)$, respectively. After divider treatment, the divider output I_{out} is shown in the formula

$$I_{\mathrm{out}} = I_{\mathrm{prob}}/I_{\mathrm{ref}} = \frac{1}{\varepsilon} I_0(v) \cdot \exp[-\alpha(v)CL]/I_0(v) = \frac{1}{\varepsilon} - \frac{1}{\varepsilon}\alpha(v)CL\,. \tag{6}$$

When the bias component $\frac{1}{\varepsilon}$ is removed from the signal and inverted (used to correct the inverting amplification output of some division chips), the final signal component $\alpha(v)CL/\varepsilon$ is proportional to the concentration of the gas to be measured.

BRD circuit is a method of full electrical noise suppression. It can provide wide band voltage and better linear characteristics in the passband, and have higher CMRR than common mode noise [11]. Its detection function is implemented based on the Ebers-Moll model, as shown in Fig. 4.

The output voltage of the BRD circuit is described by the formula

$$I(v) = G \ln\left(\frac{I_{\mathrm{ref}}}{I_{\mathrm{prob}}} - 1\right), \tag{7}$$

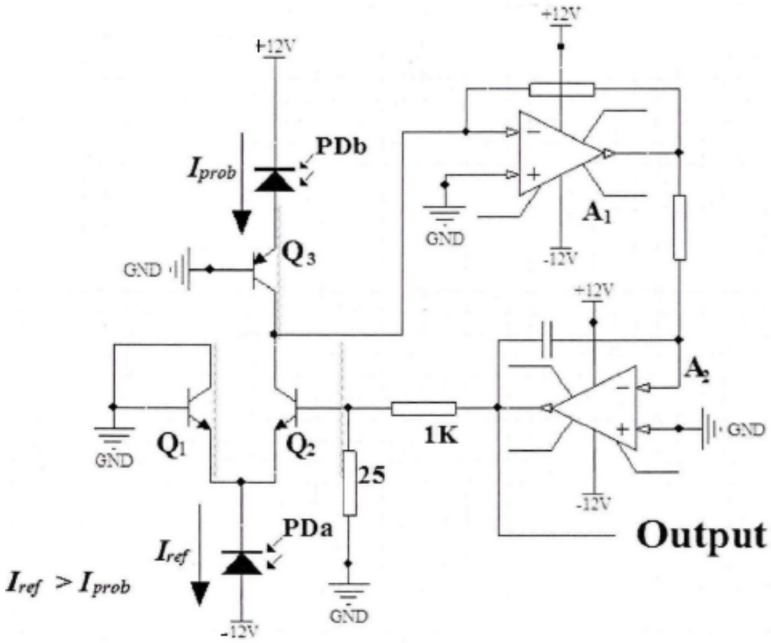

Fig. 4. Schematic diagram of BRD circuit

where G represents the overall gain of the system, and formulas (3)–(7) can be extended as shown in the following two expressions

$$I(v) = G \ln \left[\varepsilon \exp(\alpha(v)CL) - 1\right] , \tag{8}$$

$$\varepsilon \exp(\alpha(v)CL) - 1 \approx \varepsilon + \varepsilon\alpha(v)CL - 1 , \tag{9}$$

For both sides, the derivatives are obtained as follows

$$\mathrm{d}I(v) = \frac{G}{u} \mathrm{div}\ (\varepsilon + \varepsilon\alpha(v)CL - 1) , \tag{10}$$

$$\mathrm{d}I(v) = \frac{G\varepsilon}{u}\, \mathrm{d}(\alpha(v)CL) . \tag{11}$$

Here, $u = I_{\mathrm{ref}}/I_{\mathrm{prob}} - 1$.

As can be seen from formula (11), the output of the BRD circuit is directly proportional to the concentration of the gas to be measured. Therefore, we can directly calculate the amount of gas to be measured through the output voltage.

Compared with the subtraction circuit, the division circuit and the BRD circuit have normalized output, which has better inhibitory effect on the common drift of the system common mode noise and the dual optical power drift. Therefore, the application range is wider.

The scattering effects in the atmosphere include three main categories. When the radius of scattering particles is much smaller than the wavelength of light, the scattering effect is called Rayleigh scattering. When the radius of scattering particles is similar to the wavelength of light, the scattering effect is called Mie scattering. When the radius of a scattering particle grows much longer than that of the optical wave, the scattering effect is called non-selective scattering [12]. The scattering loss in single-mode fibers is generally 0.5–0.2 dB/km. In the double beam optical structure, the scattering effect in optical fiber can be minimized by controlling the difference of two fiber lengths. In this paper, the dual beam structure TDLAS system is used to control the fiber length difference between two beam propagation paths within 5 cm, and the corresponding scattering loss is only 0.000025 dB to 0.00001 dB, which can be neglected [13]. Compared to the dual beam optical structure, the scattering loss of single beam optical structure is relatively large. But because the scattering spectrum is broad spectrum, the scattering power varies very little with wavelength. Therefore, the overall attenuation of light intensity in the scanning range can be approximately considered. This effect is similar to the intensity loss effect of other optical devices that we have described later.

In practical engineering applications, bending deformation of optical fiber under stress is inevitable in optical fiber TDLAS sensing system. Generally, the optical power loss caused by fiber bending is divided into macro bending loss and micro bending loss [14].

Macro bending loss: When the fiber is bent, the transmitted light has to be kept in the same phase as the plane wave in the bent portion of the fiber. The longitudinal propagation velocity of the plane wave front is different from that of the fiber axis. The farther away from the curvature center of the bent fiber, the greater the longitudinal velocity. When the longitudinal velocity exceeds a critical value, a part of the light energy is absorbed into the cladding or passes through the cladding to become a radiation mode, and the leakage is lost, resulting in the loss of optical power. The losses in this case are known as macro bending losses. The macro bend loss of the standard single-mode fiber is given in Table 1.

Table 1. Thermophysical properties of regular fluid and nanoparticles

Bend radius of optical fiber	Bend loss (bend 1 turns)
$R = 15$ mm	<0.03 dB
$R = 10$ mm	0.039 dB
$R = 7.5$ mm	0.065 dB

Relative to macro loss, the influence of micro bend loss and light intensity is small, so the main reason is the influence of macro bending loss.

At present, most of the packaging methods for active or passive optical devices are laser welding, and the gas chamber used in this paper is the same. The two optical fiber collimators are connected together through a copper tube and then fixed by laser welding [15]. Although the laser welding technique has many advantages such as less gas, small heat affected zone, the gas chamber after the laser welding will be affected by the ambient temperature, which makes the fiber support frame

produce slight deformation, thus affecting the collimation of the collimator in the air chamber. The research shows that when the temperature changes, the fiber collimator will cause a certain degree of mismatch due to the slight deformation of the fiber support frame. The mismatch is divided into three types: off axis mismatch, slip angle mismatch, and spacing mismatch. The effect of angle offset on the coupling efficiency is greater than that of axial offset, and the coupling of fiber collimator is not sensitive to the range between them. As shown in Table 2, the insertion loss of the gas cell used in the experiment varies with the ambient temperature is listed.

Table 2. Relationship between insertion loss of air chamber and ambient temperature

Ambient temperature	Insertion loss (dB)	
	Air chamber A	Air chamber B
28 °	0.76	0.30
10 °	0.74	0.28
40 °	1.00	0.36

Through the power meter, the direct output light power of the distributed feedback semiconductor laser pigtail used in the test is measured. The relationship between the light source and the ambient temperature can be obtained, as shown in Table 3.

Table 3. Relation of the output power of distributed feedback semiconductor laser with ambient temperature

Ambient temperature	Output power of DFB semiconductor lasers (μw)
17.3 °	519.9
20.2 °	539.5
20.9 °	554.6
22.5 °	575.4
23.4 °	587.4

Fiber coupler is a very common passive optical device in the field of optical communications. It can realize the distribution and combination of the transmitted optical power between different optical fibers. The fused biconical taper (FBT) method has become the most mature and widely used method for fiber bonding devices because of its advantages of low additional loss, good directivity, and high environmental stability, simple fabrication, low cost and suitable for mass production. The so-called FBT refers that two or more bare optical fibers are put together and heated by a high temperature flame, and both ends of the fiber are stretched to both sides, and finally, a biconical cone structure is formed in the optical fiber flash melting region to form a coupler. Beam splitting ratio of single-mode fused biconical optical fiber coupler depends on the refractive index of the surrounding material of outside the melting zone. The refractive index of matter is directly related to temperature. When the surrounding material is air, the change of humidity will directly affect the refractive index of the air, and then change the beam splitting ratio of the

coupler. As shown in Table 4, the beam splitting ratio of the fiber coupler varies with ambient temperature.

Table 4. Relation of the splitting ratio of single-mode fused biconical optical fiber coupler with ambient temperature

Ambient temperature	Splitting ratio (%)
24 °	48.01
26 °	48.00
43 °	47.904

The transmission power in the optical devices is affected by the ambient temperature changes, which will undoubtedly reduce the detection performance of the TDLAS system. Because of the large number of optical devices in the TDLAS system, the change of temperature is a comprehensive effect for the whole system. When the room temperature changes from 23.8 ° to 24.8 °, the intensity of the detected beam and the reference beam intensity in the TDLAS system are increased to 102.4 % and 102.1 %, respectively. In the fourth part of the experiment and theoretical simulation, we use these two comprehensive change data to verify the detection performance of TDLAS system.

4. Result analysis and discussion

As mentioned above, the TDLAS system based on direct absorption spectrum is realized mostly on the basis of the dual beam optical structure, and the corresponding demodulation circuit has three kinds: subtraction circuit, division circuit and BRD circuit. In this part, the spectral distortion of TDLAS system based on three different demodulation circuits was investigated by theoretical simulation and experimental verification. The detection errors of three systems under the change of environmental factors (fiber bending loss and environmental temperature change) were compared.

The system used a distributed feedback semiconductor laser with a wavelength of 1368 nm. The triangular wave voltage signal with 30 Hz repetition frequency was converted into current modulation by the laser current drive circuit, and the wavelength tuning range was 240 pm. A TDLAS system employing double beam optical structures (branch of direct absorption spectroscopy) was adopted. Three demodulation circuits were used respectively for demodulation.

When the concentration of water vapor in the absorption tank is 270 ppm, the changes of absorption spectrum before and after the temperature fluctuation are shown in Fig. 5.

Because of the different amplification in the three demodulation circuits, the absorption peak of different demodulation circuits is different at the same concentration and temperature. In order to compare, the percentage of peak height change was chosen to evaluate the degree of spectral distortion and measurement error. In division circuit, the peak of water absorption spectrum increased from 520 mV to

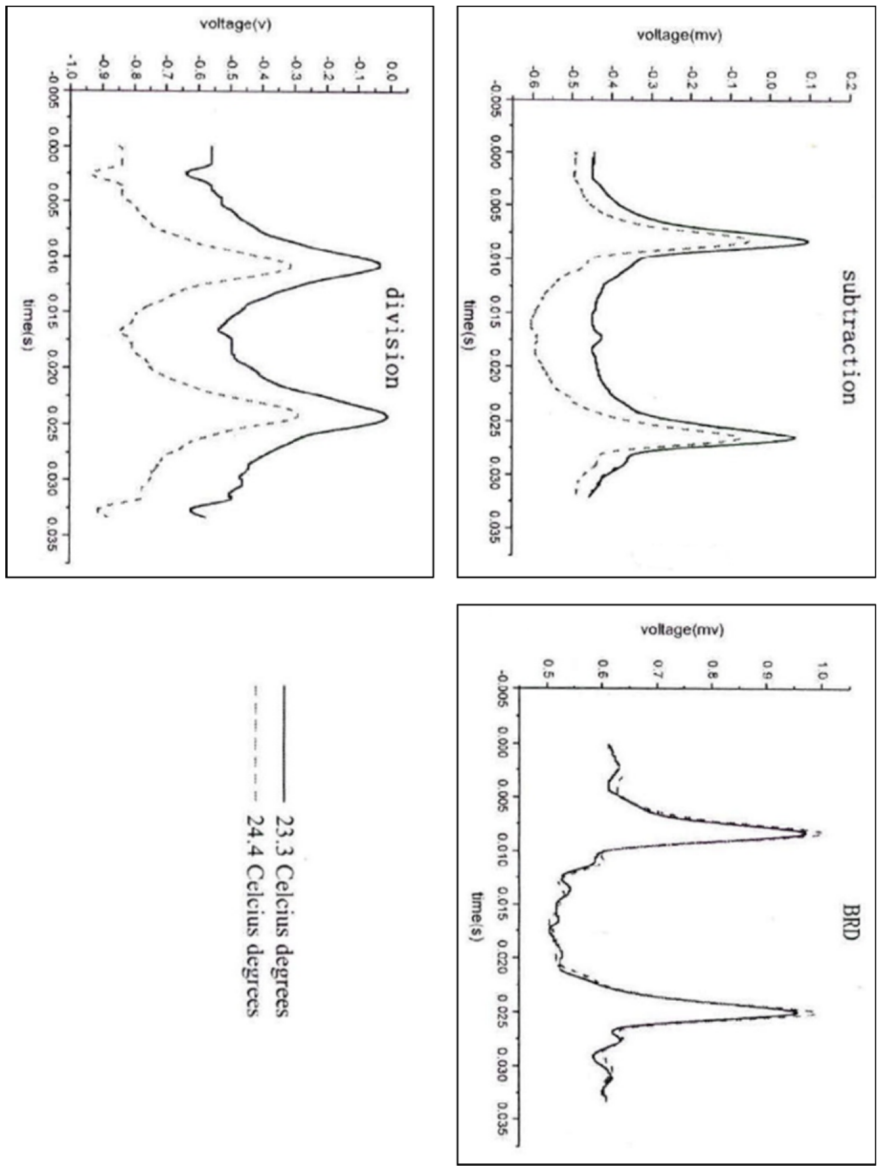

Fig. 5. Demodulation absorption line variation within 1 °C of temperature change

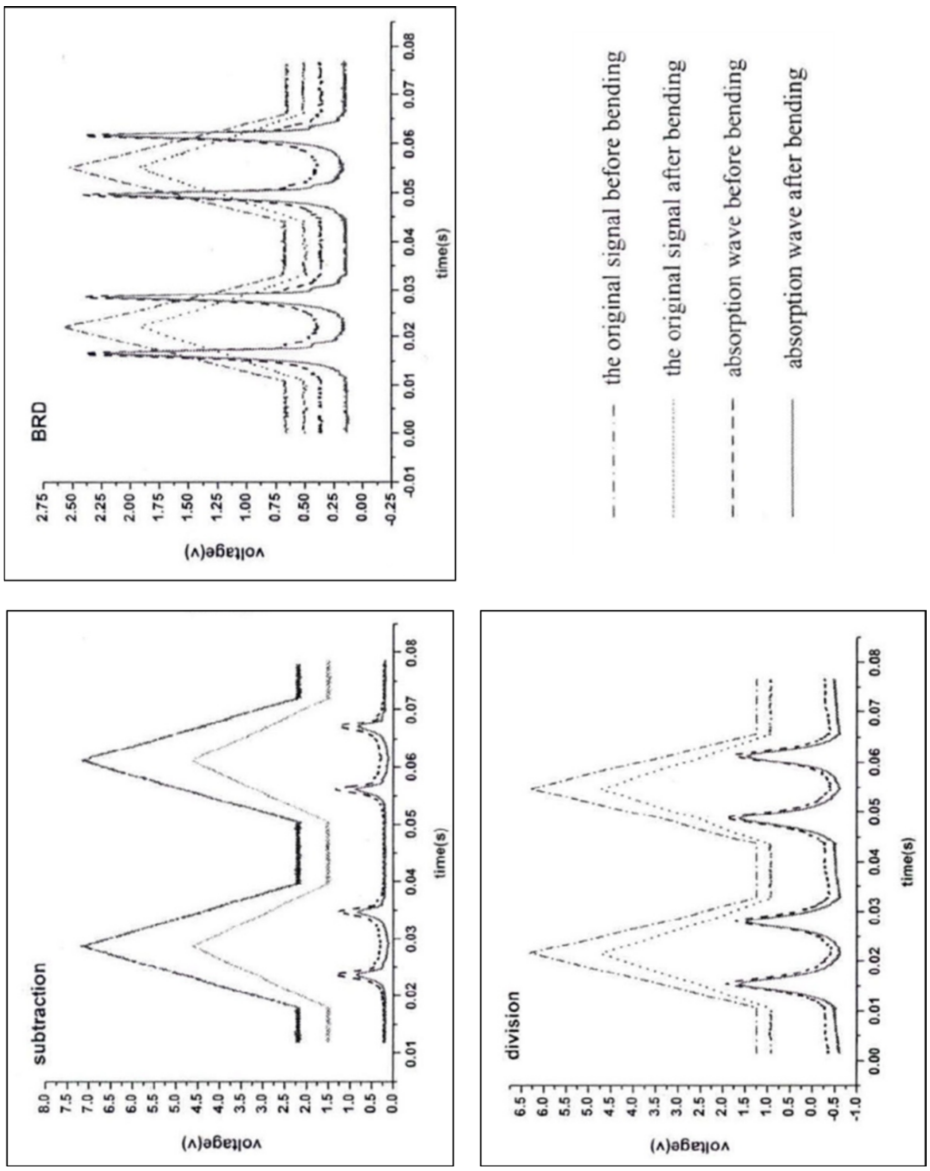

Fig. 6. Change of the absorption spectrum under the power loss of light source

528 mV, and the error was less than 1.54 %. This value was much lower than the error of the 8.82 % of the subtraction circuit (544 m–496 mV) and the error of 8.89 % of the BRD circuit (360 mV–392 mV).

When fiber bending occurred before the fiber coupler that caused the power loss of the laser light source, the water absorption spectrum of the three demodulation circuits was changed, as shown in Fig. 6.

As shown in Fig. 6, in the subtraction circuit, when the background light intensity was lowered from 4.96 V to 3.08 V (caused by the light power loss of light source), the absorption peak height was reduced by 0.44 V (1.10 V–0.66 V), and PFRR was 6.3 dB. In the BRD circuit, when the background light intensity dropped from 1.90 V to 1.42 V, the absorption peak height was decreased by 0.02 V (2.06 V–2.04 V), and PFRR was 13.8 dB. In the division circuit, when the background light intensity was attenuated from 5.08 V to 3.80 V, the absorption peak height was decreased by 0.04 V (2.10 V–2.06 V), and PFRR was 15.1 dB. It can be seen that division and BRD circuits have much higher suppression effect on light source power loss than that of the subtraction circuit. But in practice, the light intensity of two beams cannot be changed strictly. Therefore, even with the normalization, it is impossible to eliminate the measurement error caused by the power change of the light source completely.

5. Conclusion

In this paper, the physical mechanism and correction method of TDLAS spectral line distortion were studied comprehensively. Various factors causing spectral line distortion of TDLAS system were discussed, and the influence of these factors on system detection accuracy was analyzed quantitatively. The corresponding solutions were proposed respectively, and the feasibility of these schemes was verified by theory or experiment. The results show that these schemes can effectively eliminate the influence of various factors on absorption spectral line distortion, reduce the detection error of the system, and improve the detection accuracy and stability of TDLAS system. The conclusions of this study are as follows: when the ambient temperature increases by 1 °C, the detection error of division demodulation circuit is only 0.29 %, which is significantly better than the subtraction demodulation circuit (2.90 %) and BRD demodulation circuit (0.55 %). The concept of power fluctuation suppression ratio was put forward to evaluate the effect of different demodulation circuits on the power fluctuation of laser source. It was pointed out that the division demodulation circuit can provide higher detection accuracy. Through the comparison of fiber bending loss test, it was proved that the system has significant advantages in suppressing the non-absorption loss of light intensity. Although this paper has achieved good results, there are still follow-up works. For example, there has been anhydrous laser on the market, and the various indicators of similar optical devices can be tested and studied in the future.

References

[1] A. G. B. M. Sasse, H. Wormeester, A. V. Silfhout: *New approach for correction of distortions in spectral line profiles in Auger electron spectroscopy.* Surface and Interface Analysis *13* (1988), No. 4, 228–232.

[2] J. Hodgkinson, R. P. Tatam: *Optical gas sensing: A review.* Measurement Science and Technology *24* (2013), No. 1, paper 012004.

[3] A. Karpf, G. N. Rao: *Absorption and wavelength modulation spectroscopy of NO_2 using a tunable, external cavity continuous wave quantum cascade laser.* Applied Optics *48* (2009), No. 2, 408–813.

[4] L. Lathdavong, J. Shao, P. Kluczynski, S. Lundqvist, O. Axner: *Methodology for detection of carbon monoxide in hot, humid media by telecommunication distributed feedback laser-based tunable diode laser absorption spectrometry.* Applied Optics *50* (2011), No. 17, 2531–2550.

[5] M. W. Sigrist, R. Bartlome, D. Marinov, J. M. Rey, D. E. Vogler, H. Wächter: *Trace gas monitoring with infrared laser-based detection schemes.* Applied Physics B *90* (2008), No. 2, 289–300.

[6] L. Tao, K. Sun, M. A. Khan, D. J. Miller, M. A. Zondlo: *Compact and portable open-path sensor for simultaneous measurements of atmospheric N2O and CO using a quantum cascade laser.* Optics Express *20* (2012), No. 27, 28106–28118.

[7] C. G. Zhu, J. Chang, P. p. Wang, W. Wei, S. S. Zhang, Z. Liu, G. D. Peng: *Acquisition of phase-shift fiber grating spectra with 23.5 femtometer spectral resolution using DFB-LD.* Optics Express *21* (2013), No. 25, 31540–31547.

[8] L. A. Wray, J. Li, Z. Q. Qiu, J. Wen, Z. Xu, G. Gu, S. W. Huang, E. Arenholz, W. Yang, Z. Hussain, Y. D. Chuang: *Measurement of the spectral line shapes for orbital excitations in the Mott insulator CoO using high-resolution resonant inelastic x-ray scattering.* Physical Review B *88* (2013), No. 3, paper 035105.

[9] K. Duffin, A. J. McGettrick, W. Johnstone, G. Stewart, D. G. Moodie: *Tunable diode- laser spectroscopy with wavelength modulation: A calibration-free approach to the recovery of absolute gas absorption line shapes.* Journal of Lightwave Technology *25* (2007), No. 10, 3114–3125.

[10] K. Himeno, S. Matsuo, N. Guan, A. Wada: *Low-bending-loss single-mode fibers for fiber-to-the-home.* Journal of Lightwave Technology *23*, (2005), No. 11, 3494–3499.

[11] T. von Lerber, M. W. Sigrist: *Cavity-ring-down principle for fiber-optic resonators: experimental realization of bending loss and evanescent-field sensing.* Applied Optics *41* (2002), No. 18, 3567–3575.

[12] C. Li, Y. M. Zhang, H. Liu, S. Wu, C. A. Huang: *Distributed fiber-optic bidirectional strain–displacement sensor modulated by fiber bending loss.* Sensors and Actuators A: Physical *111* (2004), Nos. 2–3, 236–239.

[13] M. Kashiwagi, K. SaitohK, K. Takenaga, S. Tanigawa, S. Matsuo, M. Fujimaki: *Effectively single-mode all-solid photonic bandgap fiber with large effective area and low bending loss for compact high-power all-fiber lasers.* Optics Express *20* (2012), No. 14, 15061–15070.

[14] M. Napierała, T. Nasilowski, E. Bereś-Pawlik, P. Mergo, F. Berghmans, H. Thienpont: *Large-mode-area photonic crystal fiber with double lattice constant structure and low bending loss.* Optics Express *19* (2011), No. 23, 22628–22636.

[15] C. G. Zhu, J. Chang, P. P. Wang, B. N. Sun, Q. Wang, W. Wei, X. Z. Liu, S. S. Zhang: *Improvement of measurement accuracy of infrared moisture meter by considering the impact of moisture inside optical components.* IEEE Sensors Journal *14* (2014), No. 3, 920–925.

Received July 12, 2017